A cost-efficient seabed survey for bottom-mounted OWC on King Island, Tasmania, Australia

Remo Cossu[#1], Craig Heatherington[#2], Alistair Grinham[#3], Irene Penesis[*4], Scott Hunter [+5]

[#] *School of Civil Engineering, The University of Queensland, Australia*

[1]r.cossu@uq.edu.au

[2]c.heatherington@uq.edu.au

[3]a.grinham@uq.edu.au

[*]*National Centre for Maritime Engineering and Hydrodynamics, Australian Maritime College, University of Tasmania*

[4]i.penesis@utas.edu.au

[+]*Wave Swell Energy Ltd, 50 Camberwell Road, Hawthorn East, VIC, 3123, Australia*

[5]scott.hunter@waveswellenergy.com.au

***Abstract*— This paper presents results from a site assessment for a gravity foundation Oscillating Water Column (OWC) Wave Energy Converter (WEC) designed by Wave Swell Energy (WSE), an Australian wave energy developer. A potential candidate site for this device is the west coast of King Island, Tasmania in relatively shallow water (~ 10 m LAT). The survey included geotechnical data obtained by sub-bottom profiles, seabed imagery, benthic samples and cores with the aid of SCUBA diving as well as short-term deployment of hydromechanics instruments. Our results show that the device can be placed in an area with enough sand coverage and sufficient bearing capacity. However, the location exhibits evidence of scour and an active sediment regime, which requires a more detailed analysis of the long-term sediment transport processes and associated environmental impacts on a gravity foundation structure.**

***Keywords*—Wave energy converter, early-site assessment, seabed survey, sediment transport, geotechnical characteristics**

I. Introduction

Developers of wave and tidal energy converter systems face many challenges with respect to design, installation, maintenance and operation of offshore structures [1]. Particularly at the early stage of a site development, many questions regarding the feasibility of the site are unresolved [2]. Especially in remote offshore locations, wpave-current interaction, seabed and sediment transport characteristics, foundation and anchor systems need to be assessed during the initial stage. However, this is often challenging due to high costs associated with field measurements in dynamic marine environments, budget constraints and even the lack of best practices for field surveys. Information about cost-effective survey methods is therefore important as it contributes to developing standard procedures of site investigations.

The primary data sources for the seabed site characterization usually use a suite of instruments including: multi-beam bathymetry and backscatter, sub-bottom profiles, seabed imagery, benthic samples and cores, and sidescan sonar [e.g. 1, 3, 4, 5]. This is usually followed by detailed geotechnical and sediment dynamic studies to provide further information about site specific parameters for the safe engineering of renewable marine energy installations [3, 4, 6]. The variety of environmental and geological conditions require experience in foundation and construction methods within a rational framework [7, 8]. Thus, knowledge of the geological and geophysical characteristics of the seabed is critical to understanding the geotechnical conditions on which marine renewable conversion systems are founded or anchored.

Wave Swell Energy Ltd., an emerging Australian based wave energy company, has recently developed an enhanced concept of the traditional OWC WEC [9] which showed excellent test results and could become the next generation device with a promising wave to wire efficiency making OWC more cost-competitive [10]. The standalone full-sized OWC prototype for this study will have a footprint of roughly 20 m by20 m (Figure 1, [9]), with a nominal peak electrical generating capacity of 1 MW. A potential installation site for this OWC is located on the west coast of King Island, where the wave climate is greater than 45 kW/m [11], making it one of the best places in the world for wave energy conversion systems. However, little is known about the local seafloor conditions and geotechnical parameters at this site.

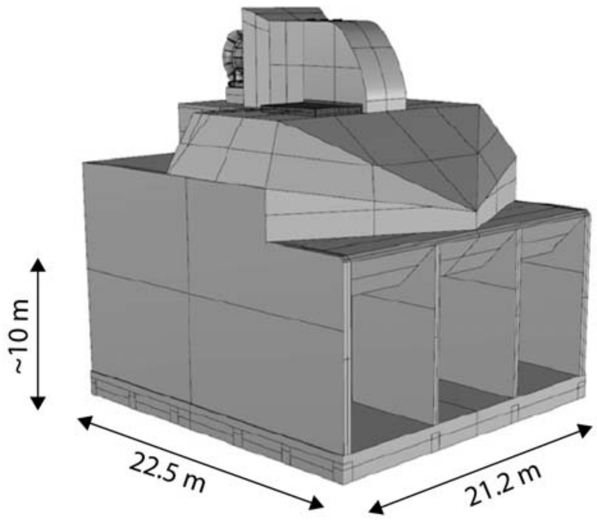

Figure 1: Dimensions of the 1MW prototpye OWC designed by Wave Swell Energy for potential deployment near King Island, Tasmania.

We report results from a seabed survey as part of an early-stage site characterisation for the OWC structure on the southwest corner of King Island, Tasmania. Field monitoring was undertaken during a relatively calm weather window in April 2017. The objective of the survey was to determine an area with sufficient sand coverage centred in approximately 10 m of water depth (MSL or 9.3 m LAT) and a minimum sand layer thickness of 1 m. The survey consisted of sediment coring and videography by SCUBA diving, sub-bottom profiling (SBP) as well as short-term deployments of acoustic Doppler current profilers (ADCPs) and turbidity sensors.

II. Methods

A. *Test Site*

King Island is situated on the western side of Bass Strait, approximately equidistant between Tasmania and the Australian mainland. The island has a population of approximately 1700 people and is powered by its own grid system consisting of wind turbines, some solar, battery storage and complemented by diesel power generation [10]. The site location was determined based on the bathymetric survey undertaken by CSIRO in early 2017 (Figure 2, bottom panel). The depth of this location was found to gently vary from 9 to 11. 3 m LAT.

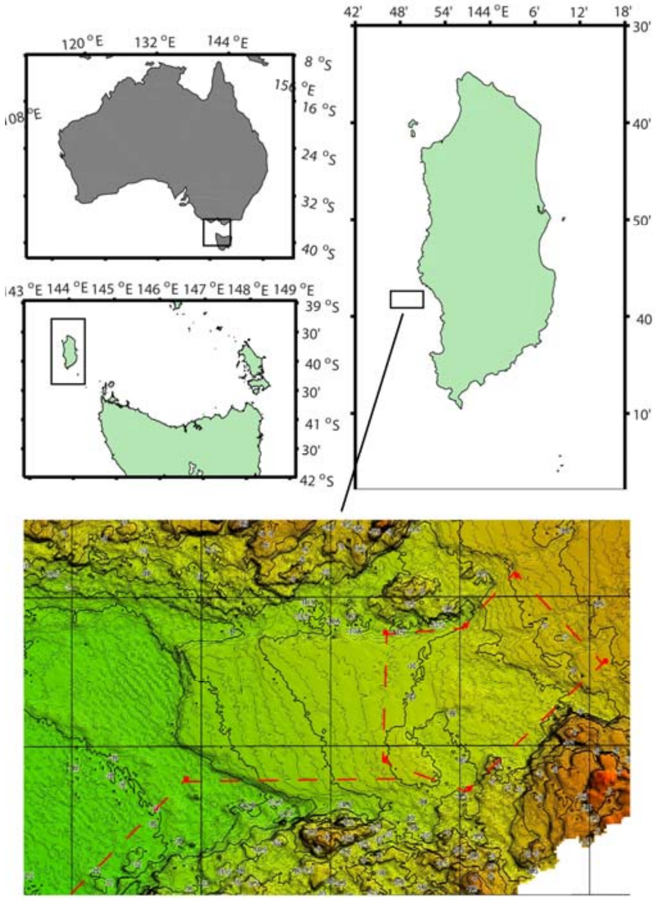

Figure 2: Location and bathymetry of survey area on King Island's west coast, Tasmania, Australia. The bathymetric survey was contacted by CSIRO in February 2018. The target area for the OWCis shown by the dashed red line.

B. *Survey Methods*

Field monitoring was undertaken during a relatively calm weather window between 3 April and 5 April in 2017. The primary activities were to deploy the field logging equipment, undertake sediment coring dives, video and sub-bottom profiling of the area of interest using the local vessel "Abstar" (8.3 m L x 2.3 m B x 1.3 m D).

Cores were taken with a piston corer which was manually operated by a diver. An initial dive was undertaken to place a star picket at a predetermined location and to deploy hydrodynamic instruments (see below) in a weighted framework. Subsequent dives occurred in succession to undertake piston core sampling. Samples were sent to the surface via a work line, extruded and the piston sampler returned to the diver. The coring locations were determined off a georeferenced star picket, the first core was taken at the picket and subsequent cores at distances of 7.5 m and 15 m in compass directions North, East, South, and West. The star picket was attached to a buoy at the surface and a handheld GPS (Garmin 72H, Garmin Ltd., Olathe, KS, USA) on board the vessel was used to georeference. All cores where the piston sampler did not penetrate more than 0.3 m were disposed of on the seabed. Some loss of sediment was possible during the retrieval of the sampler out of the seabed and compaction can occur when extruded into the larger plastic tube. Where the piston sampler was able to penetrate 1 m into the sediment, the sediment depth was greater than what could be determined via coring alone.

A series of transects were undertaken using a sub-bottom profiling system (StrataBox 3510 HD, Syqwest Inc., Cranston, RI, USA, operating at 10 kH) to further characterise the benthic surfaces within the survey area. Differences in acoustic impedance (sediment layering) was examined to detect surface expression of boulder and reef formations as well as determine the sand layer thickness. Transects were focused on mapping the potential placement site as well as a single transect along the proposed cable route.

The transducer was mounted mid-ships in a side mount configuration. Sub-bottom profiles were georeferenced using a GPS placed above the mounting bracket so no horizontal offset was required, however, a 30 cm vertical offset was required to compensate for the depth of the transducer below the waterline. Survey lines were determined based on bathymetry coordinates of the target survey as well as using buoyed droplines at the outer edges of the target area for visual reference on the surface. Transects were then performed along the sand bed and then between the reefs. SyQwest Stratabox software v.2.45 was used to record the acoustic return and initial interpretation. The Stratabox was set to a Bottom Gate Limit of 20 m depth in order to limit a 'signal noise' return via surface reverberation. Speed of sound was set later set to 1510 m/s as determined by a CTD cast. Tidal data was taken from Seal Bay AusTides prediction. An offset of 0.27 m was used to convert to LAT when importing the Stratabox acoustic data into SonarWiz 6 V6.05.0009 64-bit for post processing. During post-processing, the imported

Sub-Bottom Profile (SBP) acoustic files were laid over a basemap containing the area of interest and sediment core locations. The bottom tracking of the seabed was then processed and a 7s-wave-period swell filter was used to remove the interference of the sites large waves on the accuracy of the bottom profile. Partial trimming occurred on the SBP tracks where GPS accuracy was lost and where the transducer was warming up.

Interpretation of the results was based on several factors including in-situ diver experience, base map, backscatter information, and core sampling. This information along with a very strong single reflector under the surface was used to outline the sand layer and estimate its depth. Core sample information was georeferenced and visualised in side-view to show length of core relative to inferred stratigraphy from SBP.

To aid interpretation of the benthic surface from sub-bottom profiling data, video tows were undertaken through the potential placement area. These tows used a custom-built camera mount towed at low speed (<3 kn) with an operator maintaining a constant tow angle by manually changing the tow cable length. The camera systems utilised a forward facing, high definition underwater video camera (ASX ActionPro-X 1080P Full HD Camera) with additional lighting provided using a wide angle dive light (Bigblue VTL5500P LED Video Tech Light). Tows were georeferenced by matching the timestamps of the camera system and the vessel mounted logging GPS system. Camera position relative to the vessel was estimated from tow cable angle and water depth, sections where the water depth exceeded the towed cable length show little information about the bottom substrate and were removed from the analysis.

Geotechnical analysis was carried out on three cores to determine the following: i) soil classification; ii) density and void ratio, internal angle of friction and cohesion (if any); and iii) nominal bearing capacity. The samples taken were relatively undisturbed, meaning that most sections of the samples were firm and less disturbed while other sections were softer which could indicate a degree of disturbance. Based on these samples the strength parameters of the sand for the density, stress and water content conditions in situ were quantified. Furthermore, the bearing capacity was estimated and a sieving test was implemented to characterise the soil and sediment characteristics.

In addition to the seafloor survey, an array of instruments was deployed between Monday (03/04/2017) and Wednesday (05/04/2017) near the southern reef (143°52'55.20"E 39°59'27.60"S) to capture hydrodynamic conditions at the proposed deployment location. The array consisted of a pair HR Nortek Aquadopp ADCPs (upward and downward looking), 2 RBR Concerto CTDs (1 in fast sampling mode was attached to the ADCP frame, the other one was used for vertical profiling during the sub-bottom profiling to determine the speed of sound).

III. Results

A) Cores and sub-bottom Profiling

In total, 25 cores were retrieved (illustrated in Figure 3 and Table 1). The first coring location (easternmost black star in Figure 4) was determined to be in the eastern area of interest according to information from the bathymetry survey. However, sediment depth results proved to be unacceptable due to presence of boulder fields and very shallow sand layer coverage (< 400 mm deep, cores 1-6 in Table 1). The second coring area was extended further west. Due to difficult surface conditions and low visibility in the water, the second star picket was placed close to the northern reef (westernmost star in Figure4).

Figure 3: Photo of 25 cores retrieved from the seafloor (photo taken on King Island on the 06/04/2017).

TABLE I
CORE CHARACTERISTICS LENGTH AFTER WATER DRAINAGE, WEIGHT AND PISTON PENETRATION OF RETRIEVED CORES FROM FIGURE 3

Core number	Length [mm]	Weight [g]	Piston core penetration [mm]
1	400	1604	500
2	500	2011	500
3	360	1196	500
4	430	1613	500
5	400	1418	500
6	80	130	400
7	580	2430	1000
8	610	2386	1000
9	560	2309	800
10	640	2643	1000
11	580	2450	1000
12	520	2230	1000
13	630	2600	1000
14	580	2380	1000
15	600	2380	1000
16	650	2195	1000
17	630	2530	1000
18	610	2512	1000
19	640	2623	1000
20	610	2426	1000
21	610	2420	1000
22	550	2190	800
23	590	2420	1000
24	610	2590	1000
25	550	2310	800

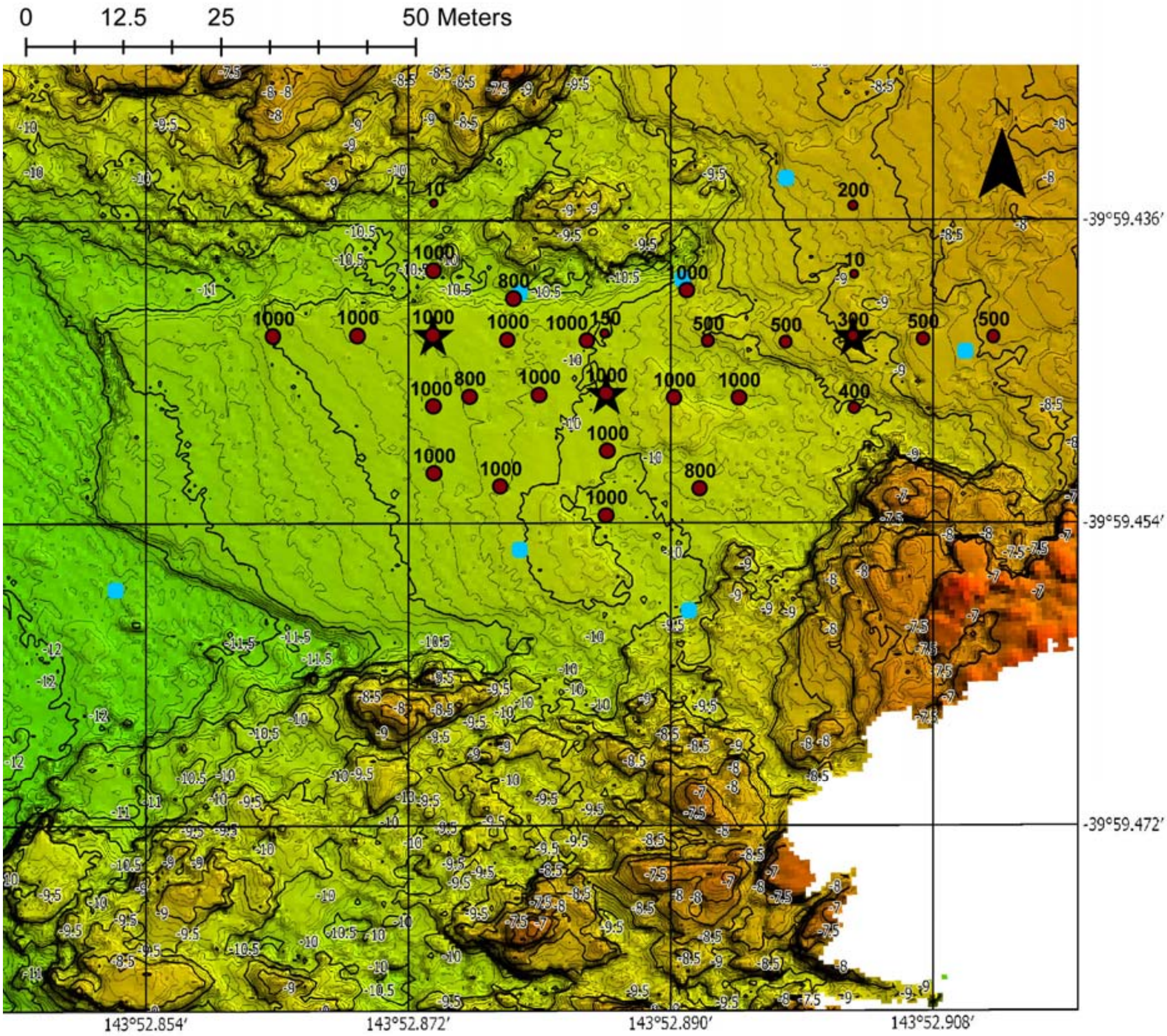

Figure 4: Location of cores taken inside and outside of the survey area. Survey polygon is depicted by the blue markers. The black stars depict the star picket centre locations which were the bases for sediment coring. Numbers and size of the cores (brown dots) reflect penetration depth (in mm).

Positive results occurred for all cores in the eastern, southern and western coring locations with sufficient sediment cover of > 1000 mm (cores 7-13 except core 9 with 800 mm, Table 1). The third coring location (depicted by the centre star in Figure 4) was placed in-between the previous two coring sites and additional four cores were taken at a distance of 15 m from centre in-between the major cardinal points (cores 14 to 25, Table 1). Two cores had a penetration depth of 800 mm while all others showed sufficient sediment cover of > 1000 mm.

Sub-bottom profiling (SBP) revealed relatively heterogeneous surface substrate with boulder and reef formations throughout the initial proposed location. A zone west of the initial location was identified as more suitable with approx. 50 m by 30 m and a minimum cover of 800 mm sand and no protruding boulder or reef structure. Figure 5 shows the vessel track lines (red solid line) for the sub-bottom survey in the target area. The SBP allowed for an accurate representation of the seafloor strata. The frequency and output power had to be calibrated to resolve the results in an acceptable parameter range (~1 m of sand depth) in post-processing. Higher frequencies have higher signal loss in sediment, but they also have higher resolution, particularly in the top layers. Decreasing power output can give less penetration in addition to less noise. The application of the 7 s swell-filter (in SonarWiz 6) was necessary to reduce the enormous signal noise from the wave swell present during the survey creating a much smoother representation of the seafloor and sub-bottom strata. Furthermore, a smaller loss of vertical detail was achieved. It is noted that the post-processing did not remove any acoustic data, nor influence the depth of the main reflector. In summary, a high resolution map of the top 2 m of sediment in a highly energetic marine environment was achieved. Where possible the physical sediment core samples were used to confirm SBP results. In total 10 core locations were synced with sub-bottom navigational paths. These 10 cores were implemented in the digitized cross section of acoustic data with an accurate representation of the piston corer penetration

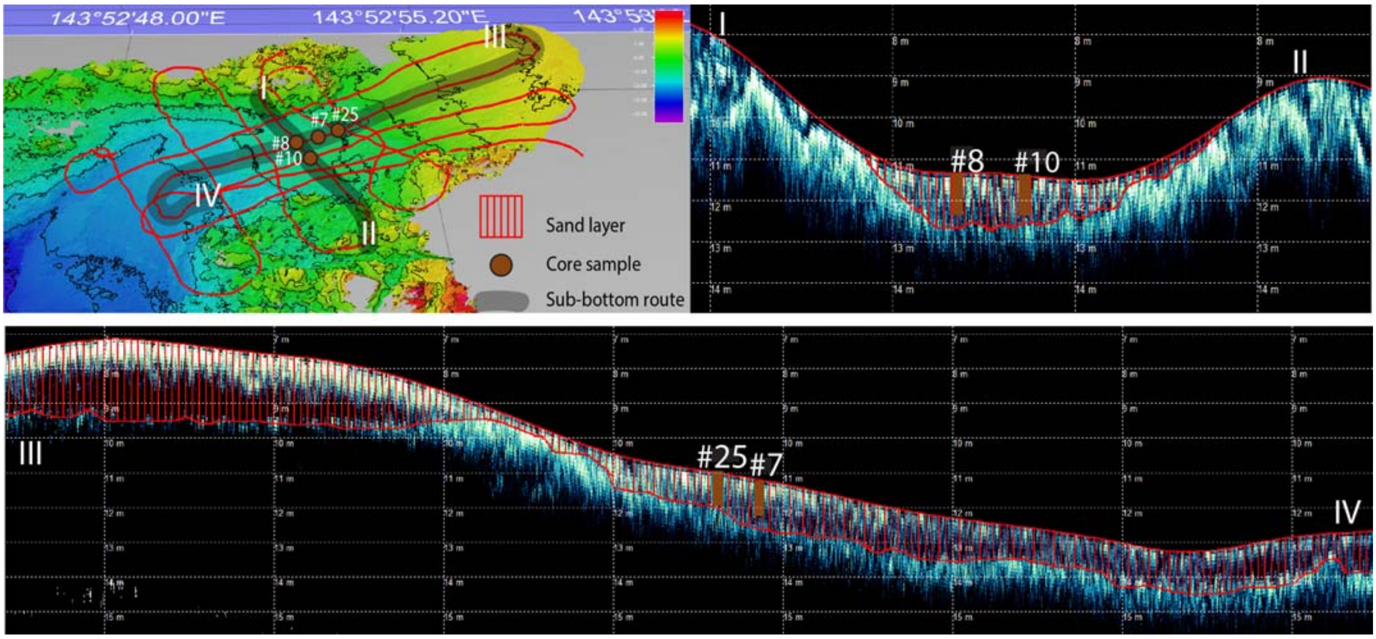

Figure 5: Transects of the SBP data. Top left panel: Overview of sub-bottom tracks in survey area. Top right panel: North-South transect. Bottom panel: East-west transect. Numbers and brown rectangles refer to cores displayed in Figures 3 and 4 and Table 1.

(not length of recovered material). This method provided confidence in the accuracy of the SBP results. Figure 5 represents the SBP trackline criss-crossing the area of interest in a roughly North-South (transect I-II) and East-West (Transect III-IV) direction. The highly variable sediment depth is evident in the panels representing the acoustic penetration depth. Further to the west (right hand side of transect III-IV) an increase in sediment depth to 1.60 m avg. can be identified. This sediment layer coverage is confirmed to 1 m in depth with sediment cores # 8 and #10 (transect I-II) before returning to a thin layer of sand in the Eastern target area and thickening again in the Western target area.

Video footage was taken on April 04 by SCUBA diver to look for seafloor characteristics, location of reefs and obstacles. Several transects were carried out from instrument string (143°52'53.583"E 39°59'27.236"S) and one from the first star picket (143°52'54.188"E 39°59'26.637"S). These transects confirm findings from the coring results showing weak sand coverage in the eastern part and a more substantial sand coverage in the western area. In particular, the videos show significant amount of boulders in the eastern part of the survey area, with an increase in density towards the northern reef. On the other hand, the western side has a more sandy character with significantly less evidence of hard substrate and boulders. The contrast of these two parts of the survey site is provided in Figures 6a and 6b. Figure 6a shows the eastern area at a depth of approx. 9 m (LAT) whilst Figure 6b is reflecting a depth of > 10 m (LAT) in the western search area.

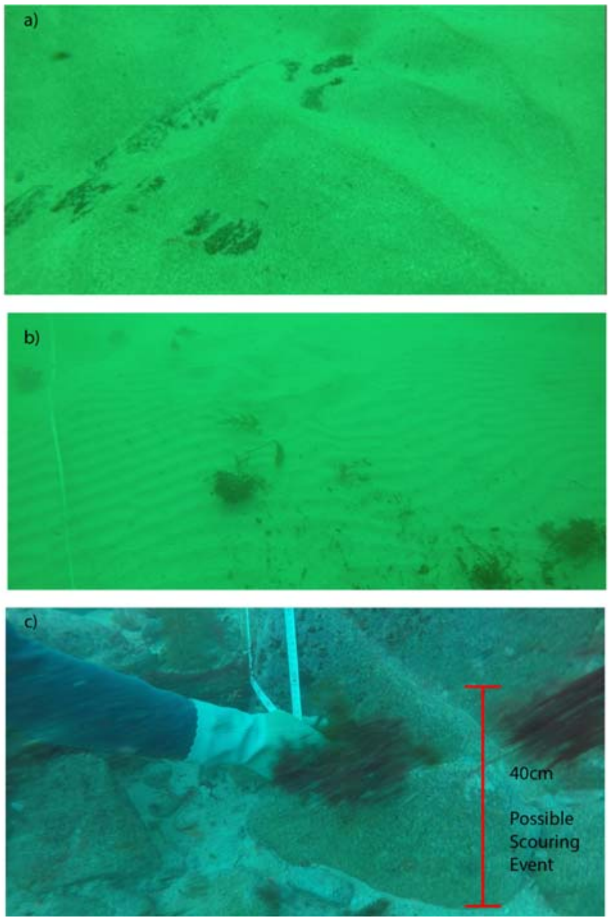

Figure 6: Snapshots of video transects in a) Eastern side and b) western side of the survey area c) Evidence of scour in northern part of the eastern area.

Figure 6c reveals another important aspect observed during site inspection video transects. The edge of the northern reef has different characteristics in relation to the apparent smoothness of boulders, sediment and encrusting algae coverage. It was evident that the shallower location had significantly less algae near the bottom 40 cm of exposed rock than the deeper area. This could be related to greater scour potential and higher impact of waves due to the smaller water depth, narrowing of valley between reefs and is consistent with findings from cores and sub-bottom data.

B) Sediment analysis

Figure 7a shows the particle size distribution of the sample taken from the seabed. The sediment consists of 90% sand and 10% gravel with no fraction in the silt or clay class. The characteristic particle diameters at 10%, 30% and 60% finer by weight are 0.21 mm, 0.41 mm and 0.7 mm, respectively. Based on these diameters, the coefficient of uniformity is Cu = 3.3 (<0.6) and the coefficient of curvature Cc = 1.1. Thus, the sample material can be classified as poorly graded Sand SP according the Unified Soil Classification System [12].
With the available data the specific gravity of the sand was tested to be G = 2.657 kg/m^3. However, it is recommended that tests on the maximum and minimum dry densities should be conducted. These tests are required to be able to quantify the in situ density conditions. Fully drained triaxial tests were conducted with three sand samples. The preparation of undisturbed samples is complex with the material retrieved from the sediment cores. Thus, to a certain degree disturbed samples were used to prepare samples at dense conditions. The corresponding Mohr Circles are given in Figure 7b and the stress paths in the p-q diagram are shown in Figure 7c. The tests define a yield surface without cohesion, and the friction angle was determined to be φ' = 41.8°. Test 3 has verified the result of Test 1. Based on the friction angle of φ' = 41.8° a first simplified estimate was used to assess the bearing capacity of offshore footings [13]. Under the following simplified assumptions: i) No eccentricity of the load, ii) Horizontal load is neglected, iii) Cohesion does not exist, and iv) Structure is sitting on the surface (shallow footing) the bearing capacity was calculated as

$$qf = Pv / BL = ½ γ' Nγ' B sy$$

with $s_y = 1 – 0.4$ B'/L (without eccentricity B' = B) and with B ≈ L we receive $s_y ≈ 0.6$. According to [14] Nγ' ≈ 100 for φ' = 41.8°. With these parameters, the bearing capacity qf was calculated for a shallow footing with a width of approximately 20m and an effective unit weight of the sediment of γ' = 10 kN/m^3 to be approximately qf = 6 MPa. If the width is reduced to 10 m due to eccentricity or loss of material under the footing qf is reduced to qf = 3 MPa. Cyclic and dynamic loading due to wave impact or water currents were not considered. Further tests with more detailed information on the in situ conditions with regard to horizontal and cyclic load, and building parameters are required for a more precise estimate of bearing capacity.

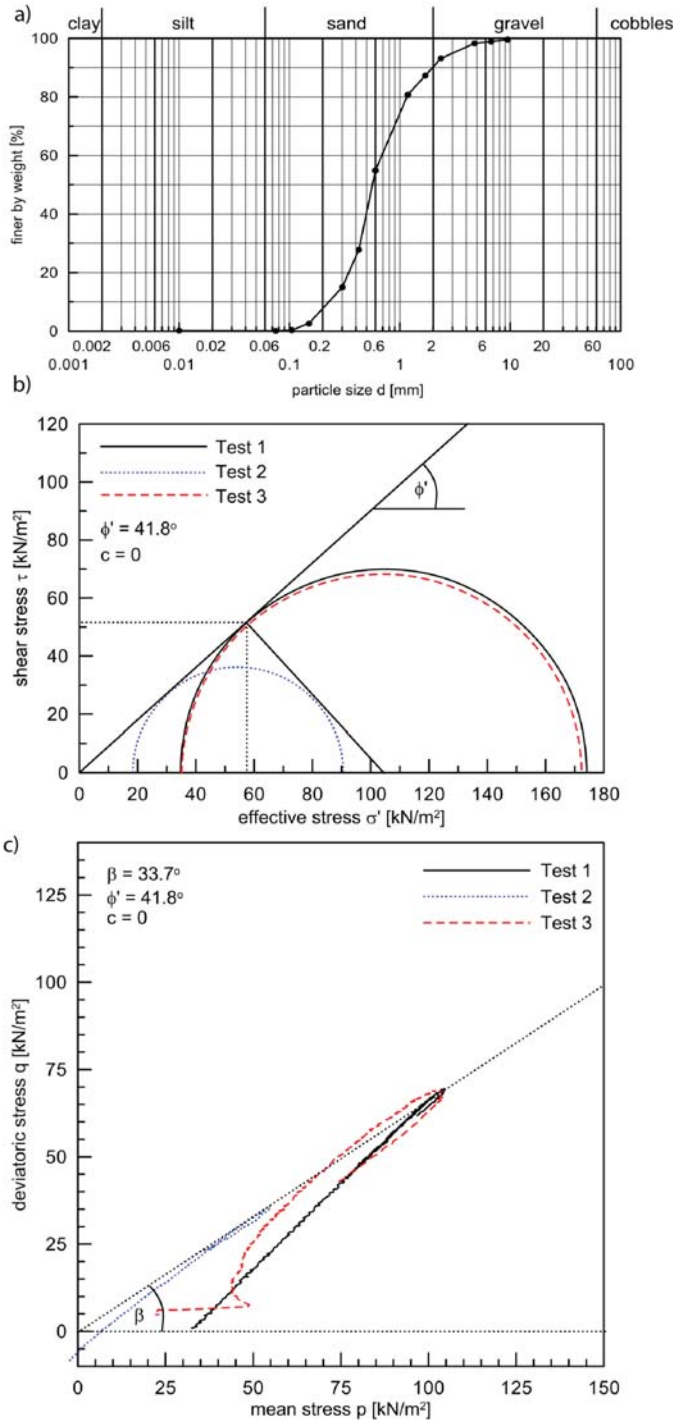

Figure 7: Sediment analysis. a) Particle size distribution of the seabed sand. b) Mohr Circle at failure state with failure plane. c) p -q diagram with yield surface

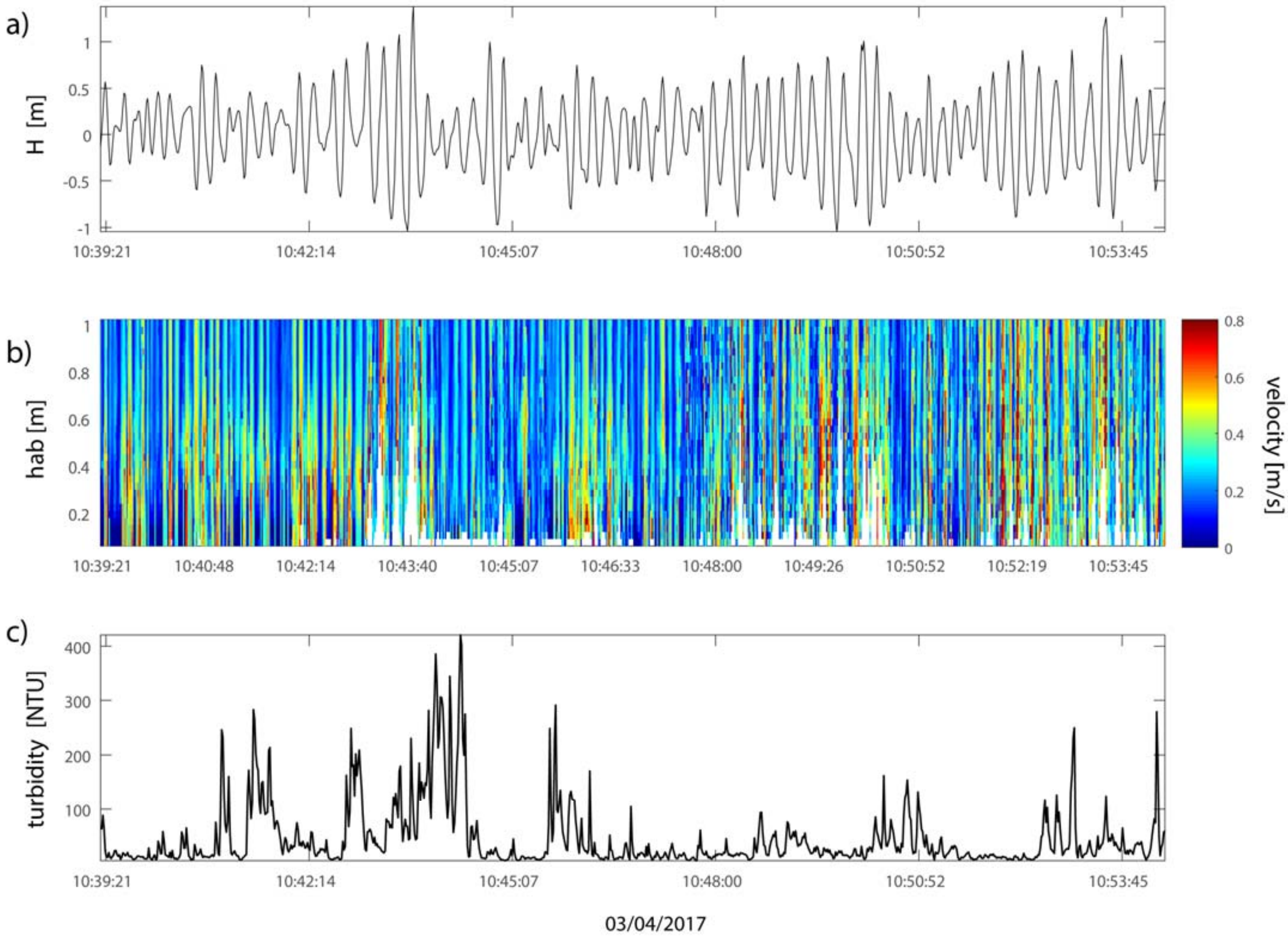

Figure 8: Hydrodynamic conditions during a 15-minute-interval representative of the energetic sea state on Monday 03/04/2017. a) Water level fluctuations from mean sea level. b) Horizontal velocity magnitudes with height above the bottom (hab). c) Recorded turbidity approximately 15 cm above the seafloor.

C) Hydrodynamics

Generally, the survey period can be split up into two periods: i) less favourable weather and wave conditions (03/04/2017) and ii) reasonably fair conditions to conduct the sub-bottom profiling, video-taping and sediment coring (04-05/04/2017). The wind on the survey days was relatively mild (< 10 knots) but the swell from previous days was still prominent during 03/04 to 04/04 morning with wave heights (H_{max}) exceeding 2 m. The wave heights are correlated to the wind conditions and showed a continuous decline between Monday morning and Tuesday afternoon. Maximum wave heights exceeded $H_{max} > 2$ m on Monday but the swell decreased to $H < 1.25$ m. Tidal currents were relatively weak with maximum velocities of 0.2 m/s throughout the water column (not shown). The tidal range during the survey was in the micro-tidal range with maximum water level differences of 0.75 m between low tide and consecutive high tide. The recorded water level fluctuations relate to the observed tidal water level fluctuations (with respect to the MSL) based on the pressure transducers of various instruments.

Figure 8 provides a description of the hydrodynamics observed during the more energetic conditions at the beginning of the survey period. For better visualization, the timeframe encompasses a 15-minute-interval between 10:40am to 10:55am on 03/04/2017. Similar conditions prevailed for the majority of the day until the wave heights started to decrease on 04/04/2017. Velocities near the seafloor reveal periodic velocity fluctuations which correlate well with passing waves (Figure 8b). Small waves led to small increases in horizontal velocities whilst large wave groups generated velocities at the order of > 1 m/s. Periods of increased velocities can be directly linked to sediment resuspension near the seafloor. Figure 8c shows turbidity levels observed approximately 15 cm above the seafloor. Particularly, large waves in passing wave trains show good agreement with elevated turbidity levels (>100 NTU) which are much larger compared to ambient turbidity levels at the order of ~10 NTU. During the passage of small waves velocities hardly exceeded

0.15 m/s with a typical logarithmic profile near the bottom. In contrast, larger waves during the observation significantly accelerate the water in the bottom meter ranging from 0.7 m/s to > 1 m/s near the seafloor. High velocity periods and increased turbidity levels are further supported by video footage and visual observations during dive operations on Monday when large waves resuspended sediments from the seafloor causing very poor visibility.

IV. Discussion

The goal of this survey was to identify the local challenges of the site to assess potential deployment locations for the OWC and the cable route to the shore. Given the favourable weather condition the preliminary site assessment for an area of approximately 1300 m^2-1400 m^2 in size could be conducted within a relatively short period of time making this realt site assessment relatively cost-efficient. This includes tasks such as acoustic sub-bottom profiling, piston-coring with divers, video transects and short-term hydrodynamic monitoring. Another important factor was access to a local vessel which guaranteed short travel (under 2 hours) to the site location. The SBP system was easy to mount over the side of the boat and enough workspace was available for diving operations and core extrusions.

Sub-bottom profiling revealed relatively heterogeneous surface substrate with boulder and reef formations throughout the proposed location. Sediment coring and video footage confirmed that the location is challenging to support full-scale seafloor structures due to boulder fields and very shallow sand layers (< 200 mm deep). However, extending the survey to slightly deeper water west of the initial location (Figures 4 and 5) revealed an area approximately 50 m x 30 m with > 800 mm of sand cover and without any boulder or reef structures.

The site exhibited a highly active sediment regime even under calm conditions. A comparison of observed water depths with a bathymetric survey two months prior to the fieldwork suggests that parts of the survey area have scoured between February and April 2017. If this is possible during a relatively mild period (February to April), further scouring in the preferred western side could occur, especially during the stormy season when waves have a greater potential to transport more sediment into or out of deeper areas. Particularly, the hydrodynamic conditions have only been analysed for a fraction of a tidal cycle (two days). This short observation period has already shown i) large fluctuations in wave height and associated near-bed velocities; and ii) the dynamic potential of sediment transport at the site. Larger waves during windy periods and storms will have a much bigger influence on the sediment transport regime but also around the structure after installation. Therefore, it is recommended that the long-term transport regime and the local scour potential under waves should be monitored for a longer period before an OWC prototype is installed at the site.

The sediment at the site consists of 90% sand and 10% gravel with no fraction in the silt or clay class with a normal bearing capacity qf = 3 MPa. Observed water velocities and bed shear stresses exceeded 1 m/s during relatively low wave energy conditions indicative of high rates of sediment transport evident by scoured sections found in the shallower part of the survey area. The limited knowledge of the wave climate and local conditions allow only a non-conservative estimate of the bearing capacity. The aforementioned parameters would aid in getting a more robust estimate and predict the behaviour of the structure under dynamic loading. Such calculations can be done with physical or numerical modelling to test mitigation measures and scour protection [15].

This survey was designed to find a target area for a single OWC device with a relatively large footprint compared to the target area. Larger areas require both longer survey times and also the use other equipment with lower risk activities compared to SCUBA diving. For instance, the use of the free-fall penetrometer (described in [1]) allows rapid geotechnical probing of the sediment type and soil mechanical characteristics. Measurements of the sediment stratification can even be used to analyse recent sediment remobilization processes [16]. The authors have successfully used BlueDrop penetrometer casts at a different renewable energy site characterization [17] with a much larger survey area. Penetration profiles help distinguish between bedrock with thin layer of sand, gravel or shell fractures [1, 18] and softer substrate. Although it is noted that penetrometer data only reflect the seabed surface, and are not a replacement for an in-depth geotechnical investigation using Cone Penetration Test or drilled sediment cores [1, 19]. However, information about uppermost substrate could aid in determining more targeted spots for sediment cores (and use of divers or expensive engines) and thus reduce survey time and costs significantly.

The conducted survey achieved the primary goal to find a sufficiently large area for Wave Swell Energy's 1MW OWC prototype. Nonetheless, the complex hydrodynamics and heterogeneity of the seabed suggest a more detailed analysis of the long-term sediment transport processes and associated impacts on a gravity foundation structure [20, 21] should be undertaken. Currently, several other sites around King Island have become a target area for testing the promising OWC design at a smaller scale.

V. Conclusions

Our objective was to determine a target area and prevailing seabed characteristics at a candidate site off the coast of King Island, Australia. The survey including sub-bottom profiling and validation by sediment coring, video imagery and sediment analysis was carried out within a short period to provide a first-order geotechnical picture of the site. An area with sand coverage of > 1 m in water depth of ~10 m was identified and seems suitable for the foundation system. However, the site exhibits also an active sediment regime and shows clear evidence of local scour. Thus, an environmental assessment of OWC foundation system should be further investigated. In particular, a more detailed analysis of the seabed-structure interaction and foundation analysis should be undertaken once the hydrodynamic conditions are better known. Such an investigation can be done with laboratory and/or numerical models which is recommended methodology for the marine renewable energy industry.

ACKNOWLEDGMENT

The authors would like to thank and acknowledge the following people for their work and help to accomplish this study. WSE and AMCS for initiating and funding this project. Grant Jordan for his help on King Island including the use of his vessel Abstar, supply of diving equipment, field operations in general and assisting with local knowledge in the planning stages. A/Prof Alex Scheuermann and the Geotechnical Lab staff at the University of Queensland for help with the analysis of the core samples. In addition, we thank the Cape Wickham Golf Club, King Island Airport Café and the local IGA tool shop for support and ad-hoc supply during the field campaign.

REFERENCES

[1] N. Stark, A.E. Hay, and G. Trowse, "*Cost-effective Geotechnical and Sedimentological Early Site Assessment for Ocean Renewable Energies*". 2014 Oceans - St. John's.

[2] R. Pelc and R. M. Fujita, "Renewable energy from the ocean," Marine Policy, vol. 26, no. 6, pp. 471–479, 2002.

[3] J V. Barry, and K.W. Conway, "*Seabed characterization for the development of marine renewable energy on the Pacific margin of Canada.*" Continental Shelf Research. 83, 45-52. 2016

[4] P. Ramsay, W. Miller, and D. Murrell, "*Supporting renewable energy projects using high resolution hydrographic and geophysical survey techniques, Garden Island, Western Australia.*" Underwater Technology, vol. 33: pp. 229-237, 2016

[5] J. A. Goff, B. J. Kraft, L. A. Mayer, S.G. Schock,, C. K. Sommerfield, H. C. Olson, S. P. S Gulick, and S. Nordfjord, "*Seabed characterization on the New Jersey middle and outer shelf: correlatability and spatial variability of seafloor sediment properties.*" Marine Geology, vol 209, pp. 147-172, 2004.

[6] M. A. Chatzigiannakou, I. Dolguntseva, and M. Leijon, "Offshore Deployments of Wave Energy Converters by Seabased Industry AB." Journal of Marine Science and Engineering, vol. 5, 2017.

[7] J.A. Schneider, M.L. Maynard, and M. Senders, "*Geotechnical engineering for offshore wind turbine foundations.*" Sea Technol., vol. 51, pp. 29–33, 2010.

[8] L. Chen, and W.-H. Lam, "*Methods for predicting seabed scour around marine current turbine.*" Renewable and Sustainable Energy Reviews vol. 29, pp 683-692, 2014.

[9] J. Brown, (2017, January). Available: http://waveswellenergy.com.au/technology/.

[10] A. Fleming, G.J. Macfarlane, S. Hunter, and T. Denniss, "*Power Performance Prediction for a Vented OWC Wave Energy Converter with a Unidirectional Air Turbine Power Take-off.*" Proceedings of the 12th European Wave and Tidal Energy Conference, Cork, Ireland, 27 August – 2 September, Cork, Ireland, pp. 1204-1 – 1204-7.

[11] M. A. Hemer, and D. A. Griffin, "*The wave energy resource along Australia's Southern margin.*", Journal of Renewable and Sustainable Energy, vol. 2, no. 4, Aug. 2010.

[12] M. Sperazza, J.N. Moore, and M.S. Hendrix, "*High-resolution particle size analysis of naturally occurring very fine-grained sediment through laser diffractometry.*" Journal of Sedimentary Research, vol. 74, 736-743, 2004.

[13] L. Bjerrum, "*Geotechnical problems involved in foundations of structures in the North Sea.*" Géotechnique, vol. 23, pp. 319-358, 1973.

[14] J.B. Hansen, "*A revised and extended formula for bearing capacity*". Bulletin 28, pp. 5-11. Copenhagen: Danish Geotechnical Institute, 1970.

[15] J. E. Heath, R. P. Jensen, S. D. Weller, J. Hardwick, J.D. Roberts, and L. Johanning, "*Applicability of geotechnical approaches and constitutive models for foundation analysis of marine renewable energy arrays.*" Renewable & Sustainable Energy Reviews, vol. 72, pp. 191-204, 2017.

[16] N. Stark and A. Kopf, "*Detection and quantification of sediment remobilization processes using a dynamic penetrometer.*" in Proceedings of the IEEE/MTS Oceans'11.

[17] (2018) Tidal Energy in Australia website. [Online]. Available: http://austen.org.au/index.php/2018/03/20/update-on-the-banks-straight-field-campaign/

[18] N. Stark, A. E. Hay, G. Trowse, and A. Kopf, "*Geotechnical investigation of Grand Passage, Nova Scotia, with regard to sediment mobility and the installation of tidal turbines.*" in Proceedings of the European Wave and Tidal Energy Conference, Aalborg, Denmark, September 2013, 2013.

[19] P. Robertson, "*Soil classification using the cone penetration test.*" Canadian Geotechnical Journal, vol. 27, pp. 151–158, 1990.

[20] B. M. Sumer, "*Flow–structure–seabed interactions in coastal and marine environments.*" Journal of Hydraulic Research, vol. 52, pp 1-13. 2014.

[21] B. Mutlu Sumer, F. Hatipoglu, J. FredsØE, and S. Kaan Sumer, "*The sequence of sediment behaviour during wave-induced liquefaction.*" Sedimentology, vol. 53, pp. 611-629, 2006.